Journal of Applied Polymer Science

Structure, Electrical, Dielectric, and Optical Investigation on Polyvinyl Alcohol/Metal Chloride Nanocomposites

N. M. Shash,[1] H. Khoder,[1] F. Metawe,[2] A. A. Negm[1]

[1]Department of Physics, Faculty of Science, Benha University, Benha, Egypt

[2]Department of Basic Science, Faculty of engineering, Benha University, Shoubra, Egypt

Correspondence to: N. M. Shash (E-mail: nabilshash10@hotmail.com)

ABSTRACT: Different concentrations of metal chlorides/polyvinyl alcohol nanocomposites have been prepared by the typical solvent cast technique. The prepared samples were investigated by different techniques such as X-ray diffraction, differential scanning calorimetry, and scanning electron microscope. DC and AC conductivities are examined at different temperatures and frequencies. An activation process was found in the DC conductivity versus temperature relation and the activation energy was calculated. The AC conductivity obeyed the ω^S power law. The behavior of S with temperature was studied. Various dielectric parameters such as dielectric constant (ε'), dielectric loss (ε'') and loss tangent (tan δ) have been determined in the temperature range 303–443 K at different frequencies. The dielectric parameters were found to decrease with increasing frequency. The study of dielectric relaxation as a function of temperature at constant frequency shows two relaxation mechanisms. The optical band gaps and band tails were estimated from the measured absorption spectra. The applied photon energy found to affect the observed optical band gaps. © 2013 Wiley Periodicals, Inc. J. Appl. Polym. Sci. 129: 2796–2805, 2013

KEYWORDS: dielectric properties; nanostructured polymers; optical properties

Received 1 October 2012; accepted 6 January 2013; published online 4 February 2013

DOI: 10.1002/app.38998

INTRODUCTION

Polymer nanocomposites represent a new alternative to conventionally filled polymers. Because of their nanometer sizes, filler dispersion nanocomposites exhibit markedly improved properties when compared to the pure polymers or their traditional composites. Polymers that contain transition metal complexes endow many peculiar properties such as nonlinear optical properties and electronic conductivity. They are promising candidates for their use in various applications, including chemical sensor, electroluminescent devices, electrocatalysis, batteries, and memory devices.[1]

Polyvinyl alcohol (PVA) which is water soluble polymer was selected as the backbone material of the composite samples. PVA which is a semicrystalline polymer exhibits very important applications due to the role of OH group and hydrogen bonds.[2] Further, it can be used as a medical material due to its compatibility to the living body. It has been shown to be a good host for various fillers.[3,4] Many Ni(II), Co(II), and Mn(II) compounds are paramagnetic, due to the presence of two unpaired electrons on each metal center which may be a source for electrical and magnetic properties of the transition metal halides. The most stable oxidation state for these metals is +2. $NiCl_2$, $MnCl_2$, and $CoCl_2$ were selected as the preferred and best characterized filler materials due to their low cost, water solubility and the easy attachment of chlorides with polymer chains. Two main methods can be used to prepare polymer nanocomposites: dispersion of preformed inorganic fillers and in situ generation of inorganic dispersion of preformed inorganic fillers and in situ generation of inorganic fillers.[5–7]

The aim of the present work is to study the effect of addition of $NiCl_2$, $MnCl_2$, and $CoCl_2$ in nanosize on the structural, dielectric and optical properties of PVA.

EXPERIMENTAL

Materials and Samples Preparation

PVA $(C_2H_4O)_n$ (where $n = 1800$) in form of grains was used in preparation of samples. Nickel chloride (hexa hydrate) ($NiCl_2{\cdot}6H_2O$), cobalt chloride (hexa hydrate) ($CoCl_2{\cdot}6H_2O$) and manganese chloride (tetra hydrate) ($MnCl_2{\cdot}4H_2O$) are the metals salts and cetylpridinium bromide monohydrate as the surfactant ($M_w = 402.47$ g/M). The bidistilled water was used as solvent.

The same steps were used to prepare metal chlorides/PVA nanocomposites, PVA solution was prepared via adding distilled

water to solid PVA and stirred by a magnetic stirrer at 333 K for 2 h. When the temperature dropped to the room temperature, 30 mL of aqueous solution of cetylpridinium bromide (0.002*M*) was added to the PVA solution and allowed to stir together for about 20 min. Then, metal chloride solution with the desired concentration was added dropwise into the reaction vessel, followed by stirring for 2 h. The prepared composite was directly casted in a Petri- glass dish and kept at room temperature for 1 week. Samples of PVA contain 41.6, 32.2, 19.2, and 4.5 wt % of $CoCl_2$, $NiCl_2$, and 37.2, 28.3, 16.5, and 3.8 wt % of $MnCl_2$ were obtained.

Tools of Analysis

To investigate the nature of the polymer samples, differential scanning calorimetry (DSC) thermograms were carried out using a thermoanalyzer (Shimadzu DSC-50) with a measuring temperature range of 293–443 K and a heating rate of 5 K/min. X-ray diffraction (XRD) patterns for the prepared samples were recorded with a Philips X-ray diffractometer using monochromatized $CuK_{\alpha 1}$ radiation of wavelength 1.54056 Å from a fixed source operated at 45 kV and 9 mA. The morphology of the samples was observed by using Philips XL 30 scanning electron microscope (SEM), operating at an accelerating voltage of 30 kV magnifications 10×–400× and resolution for *W* (3.5 nm). For DC electrical conductivity measurements, samples in the form of rectangular sheets (0.3-mm thickness and 0.33 cm^2 an effective area) were used. The used area for measurements was coated with silver conducting paint, which showed for good contact. The measured sample was fixed between two brass electrodes and heated in an electrical furnace in the temperature range 303–443 K. The rate of heating was adjusted to be 1 K/min, using a digital temperature controller. The current flowing through the sample was measured with a Kithely 485 programmable electrometer. AC conductivity and dielectric properties of the samples were performed in the temperature range 303–443 K over the frequency range 100–100 KHz using PM 6304 programmable automatic RLC meter. The UV–vis spectra were carried out at room temperature using a Perkin Elemer lambda 3B (UV–vis) spectrophotometer in the wavelength range of 200–900 nm.

RESULT AND DISCUSSION

Characterization

XRD Spectra. XRD pattern of the pure and metal chloride doped PVA is shown in Figure 1. A broad peak was noticed at $2\theta \approx 19.5°$ for pure PVA which can be assigned to the Van der Wall distance of 4.5 ≈ 5 Å.[8] However, for doped samples, this peak has been found to increase in broadness and gradually disappears. This clearly shows the increased amorphous nature of PVA film with increase in salt concentration. This result can be interpreted by considering the Hodge et al.,[9] which establishes a correlation between the intensity of the peak and the degree of crystallinity. This broad nature of peak and its disappearance from the polymer composites suggests the amorphous nature of the polymer composite. Conversely, few new peaks appears for the highest concentration doped samples which were corresponding to the nature of metal chloride.

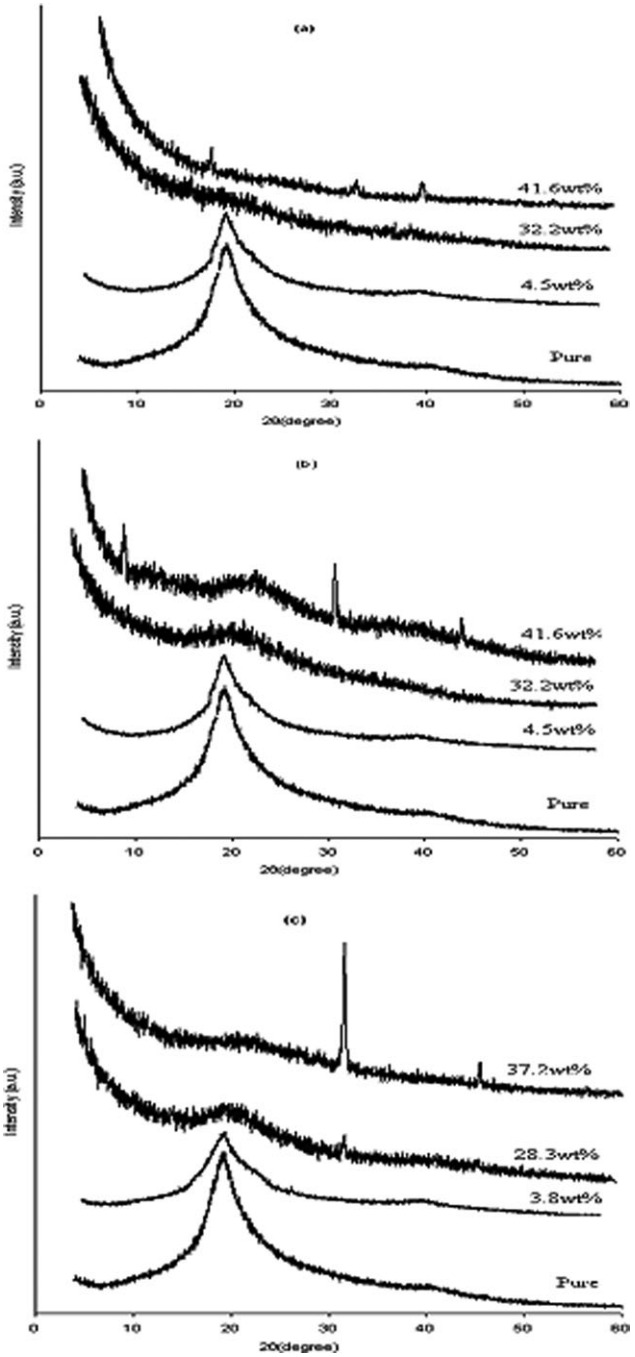

Figure 1. XRD pattern for the prepared samples (a) PVA/$CoCl_2$, (b) PVA/$NiCl_2$, and (c) PVA/$MnCl_2$.

The crystalline regions are connected to amorphous regions in which the molecular chains of the polymer are irregularly folded. The interaction of hydroxyl groups present as side groups in PVA with the metal ions has a significant influence on the polymer chain mobility and on the structure. The average crystallite sizes D of metal chloride crystals are evaluated utilizing the XRD for all composites with Scherrer's relationship of the form,[10]

$$D = 0.89\lambda/(\mathrm{B}.\cos\theta) \quad (1)$$

Table I. Microstructure Data from X-ray of PVA/Metal Chloride Composites

Metal chloride	Content (wt %)	Crystallite size *D* (nm)
$CoCl_2$	32.2	54.7
	41.6	29.8
$MnCl_2$	28.3	31.8
	37.2	35.8
$NiCl_2$	32.2	68.4

where 0.89 is the Scherrer constant, λ is the wavelength for the used X-ray, B is the breadth of the pure diffraction profile and θ is the incidence angle of the X-ray. The wavelength of the X-ray is 0.154 nm for Cu-Kα. The derived values of D are given in Table I.

Morphological Studies. Figure 2 shows the SEM micrograph of the surface of pure and filled PVA polymer samples. From this figure, it is clear that it has a uniform surface morphology revealing a rather smooth surface for pure PVA. Figure 2(b) for 41.6 wt % of $CoCl_2$/PVA filled polymer sample as a representative one shows that $CoCl_2$ has great effect on the morphology and the particle size of the polymer, since $CoCl_2$ particles appears to be highly dispersed in the polymer matrix in the form of spherical shapes with small diameter in the range of 53.6–87 nm with good homogeneity. Figure 2(c) for 41.6 wt % of $NiCl_2$/PVA filled polymer sample as a representative one shows that there are some new shapes with different sizes in the range of about 53.6–80.4 nm appeared as bright fine wires. Also, these uniform distributed bright wires on the backscattered images shown in the figure seem to be agglomerates of nickel chloride particles. This change confirmed the interaction and complexation between the filler and the polymer. Figure 2(d) for 37.2 wt % of $MnCl_2$/PVA filled polymer sample as a representative one shows that $MnCl_2$ has great effect on the morphology of the polymer. There are different shapes. However, absence of pores in the structure shows that there is a very strong interaction among the particles. Finally, this difference that noticed between the crystal sizes obtained from XRD and that from SEM may be due to aggregation of particles.

DSC. Figure 3 shows the DSC thermograms for pure and PVA doped with 32.2 wt % of $CoCl_2$ and $NiCl_2$, 28.3 wt % of $MnCl_2$ as a representative diagrams for the investigated samples. The observed transitions in pure and all the doped samples can be assigned as that the exothermic peak for all samples at about 323 K could be due to a small amount of moisture, which is resent in the conventional sample unless it is carefully vacuum dried.[11] Figure 3(a) shows endothermic transition at about 338 K attributed to glass transition temperature (T_g) relaxation process for PVA. Then a broad transition around 374–382 K may be assigned to the relaxation associated with the crystalline regions (T_c).[12] In $CoCl_2$/PVA sample the position of T_g shifted toward higher temperatures with respect to the pure PVA. There are new peaks around 353–361 K for $NiCl_2$/PVA sample which may be due to the polymer and filler interaction. The two transitions associated with T_g and T_c slightly shifted toward higher temperatures for $MnCl_2$/PVA sample with respect to the pure PVA, suggests the increase in thermal stability.

Electrical Properties

DC Conductivity. The temperature dependence of σ_{dc} of all investigated samples in the temperature range of 303–443 K is depicted in Figure 4. According to Figure 4(a) for PVA/$CoCl_2$ the DC conductivity seems likely to increase with increasing

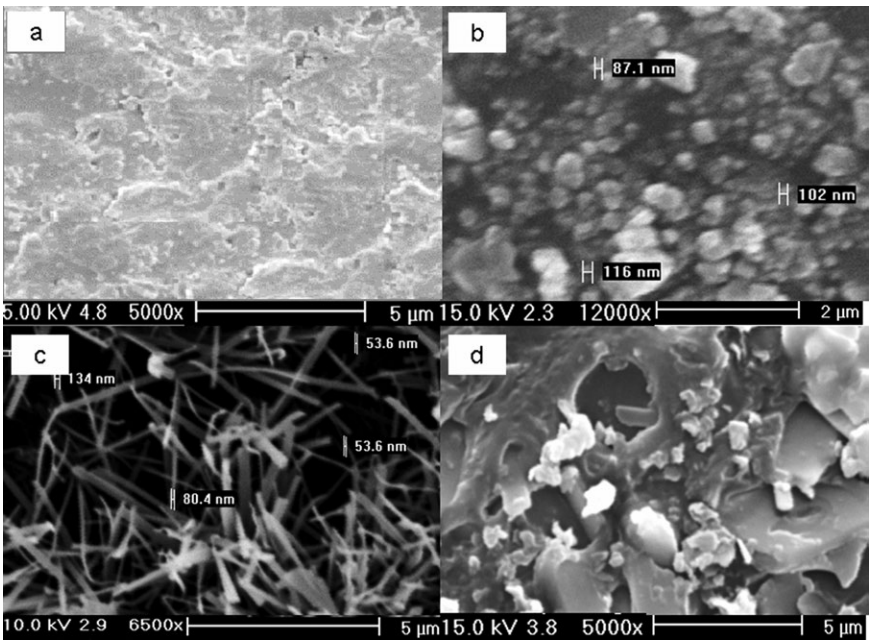

Figure 2. SEM micrograph of (a) pure PVA and PVA/ metal chloride: (b) PVA/41.6 wt % $CoCl_2$ with, (c) PVA/41.6 wt % $NiCl_2$, and (d) PVA/37.2.6 wt % $MnCl_2$.

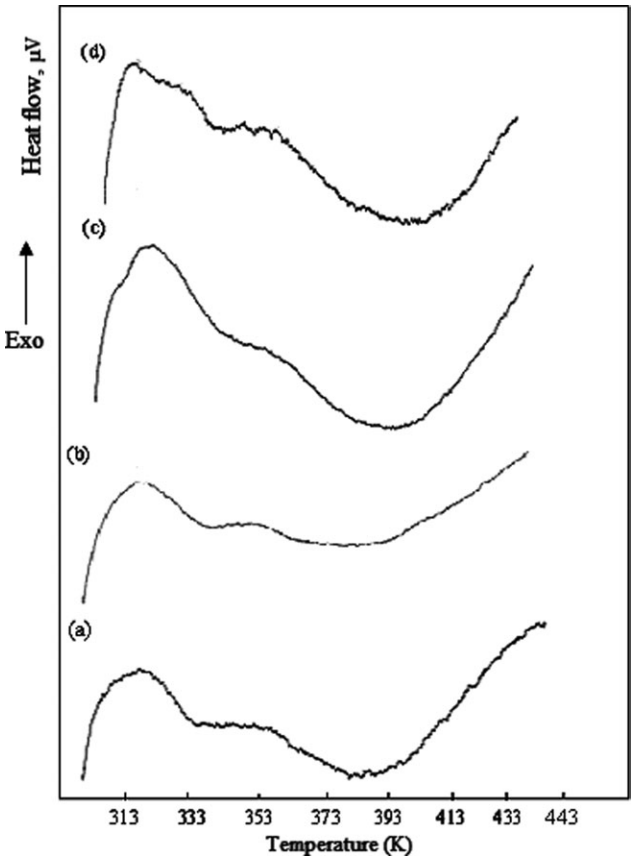

Figure 3. DSC thermograms of (a) pure PVA, (b) PVA/32.2 wt % $CoCl_2$, (c) PVA/28.3 wt % $MnCl_2$, and (d) PVA/32.2 wt % $NiCl_2$ doped samples.

temperature. Similar behavior can be noticed for both PVA/$NiCl_2$ and PVA/$MnCl_2$ doped samples composites as shown in Figure 4(b,c). Such variation in the conductivity against temperature indicates that the conduction is thermal activated process. From the linear part of the curves, the activation energy was calculated according to Arrhenius relation,[13]

$$\sigma_{\mathrm{dc}} = \sigma_o \exp\left(-\mathrm{E}_a \Big/ \mathrm{K_B T}\right) \tag{2}$$

where σ_o is temperature independent constant, E_a is the activation energy, K_B is Boltzman constant and T is the absolute temperature. A probable explanation for the increase of σ_{dc} with temperature is attributed to polymer chain mobility and activation of metal chlorides phases in each composite.

The estimated values of E_a by fitting are listed in Table II. The relative low values of E_a can be accounted for the amorphous nature of the composites which enhanced the mobility of charge carriers. Also, this reduction in the activation energy may be due to the electrostatic interaction between negative charged hydroxyl group and positive metal ions.[14]

The $\sigma_{\mathrm{dc}} - T$ relation can be analyzed According to Mott model,[15]

$$\sigma = \sigma_o \exp\left[-(\mathrm{T}_o \Big/ \mathrm{T})\right]^{1/4} \tag{3}$$

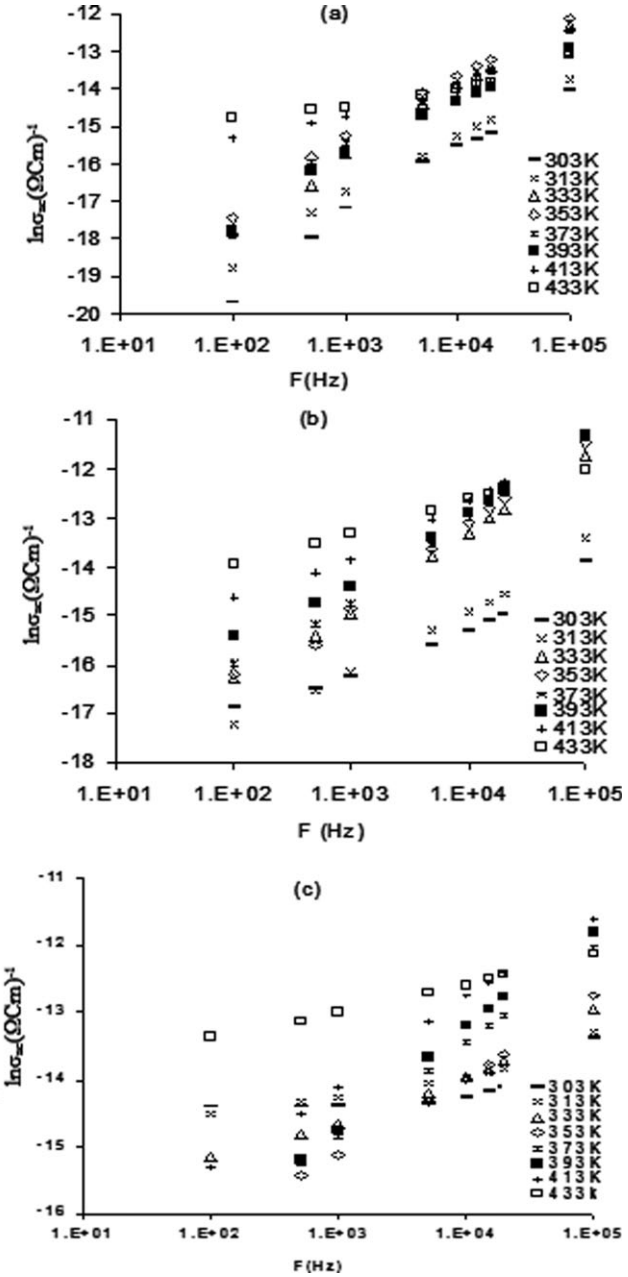

Figure 4. Temperature dependence of the DC Electrical conductivity for (a) PVA/$CoCl_2$, (b) PVA/$MnCl_2$, and (c) PVA/$NiCl_2$.

where σ_o is a moderately temperature-dependent pre exponential factor and T_o is the characteristic temperature that determines the thermally activated hopping among localized states at different energies and considered as a measure of disorder and given by,[16]

$$T_o = \lambda_D \alpha^3 \Big/ K_{\mathrm{B}} \mathrm{N}(\mathrm{E}_f) \tag{4}$$

where $\lambda_D = 18.1$ is a dimensionless constant, $\alpha = 10$ Å is the inverse rate of fall of the wave function and $N(E_f)$ is the density of state at the Fermi level.[14] Both T_o and $N(E_f)$ were calculated from eqs. (3) and (4) for all investigated samples listed in Table II. The decrease of T_o with increasing metal chloride content is

Applied Polymer SCIENCE

Table II. The Calculated Values of E_a (eV), E_h (eV), T_o, and $N(E_f)$ for all Investigated Samples

PVA/metal chloride	Metal chloride content (wt %)	E_a (eV)	E_h (eV)	$N(E_f)$ (cm^{-3}/eV)	T_o (K)
PVA/$CoCl_2$	4.5	0.64	0.69	1.26E+16	1.67E+10
	19.2	0.51	0.52	3.05E+16	6.89E+9
	32.2	0.5	0.47	3.26E+16	6.43E+9
	41.6	0.46	0.46	4.69E+16	4.48E+9
PVA/$NiCl_2$	4.5	0.63	0.65	1.47E+16	1.43E+10
	19.2	0.27	0.28	4.79E+17	4.39E+8
	32.2	0.26	0.27	4.91E+17	4.28E+8
	41.6	0.26	0.27	4.92E+17	4.26E+8
PVA/$MnCl_2$	3.8	0.42	0.43	7.53E+16	2.79E+9
	16.5	0.27	0.26	3.82E+17	5.5E+8
	28.3	0.29	0.31	3.03E+17	6.03E+8
	37.2	0.28	0.31	3.49E+17	6.01E+8

attributed to the effect of dispersion and coalescence of filler with polymer matrix. Hereafter, the increase of $N(E_f)$ with increasing metal chloride content is attributed to increase the capacity of conductive networks with strong localization.[14] The marked increases of $N(E_f)$ with decreasing of T_o for all PVA metal chloride nanocomposites samples indicate that the conducting paths change the geometrical characteristics (i.e., interchain distance among conductive sites) inside the polymer matrix with increasing metal chloride content.[17]

To check the type of conduction mechanism in PVA metal chloride nanocomposites, the hopping energy E_h, can be calculated according to the following formula,[18]

$$\sigma\sqrt{\mathrm{T}} = \mathrm{A}\exp - \left(E_h \Big/ K_{\mathrm{B}}\mathrm{T}\right) \tag{5}$$

where A is a constant. The estimated values of E_h as a function of metal chloride content for all prepared samples are listed in Table II. The values of E_h is quite close to the value of E_a, this means that the conduction mechanism in PVA metal chloride nanocomposites is governed by small polaron hopping conduction mechanism.[18]

AC Conductivity. Figure 5 show the dependence of AC conductivity, σ_{ac}, on the frequency at different ambient temperature for PVA/41.6 wt % $CoCl_2$, $NiCl_2$, and PVA/37.2 wt % $MnCl_2$ nanocomposites as representative diagram. The rise of conductivity upon increasing frequency and temperature is due to the tremendous increase of the mobility of charge carriers.[19] The number of charge carriers, which have high relaxation time due to higher energy barrier and respond in low frequency regime, might be less in number; hence, the conductivity is lower at lower frequencies. However, the number of charge carriers with low barrier heights is bigger and they responded easily with high frequency and showed higher conductivity at higher frequencies. This behavior suggests that the hopping mechanism

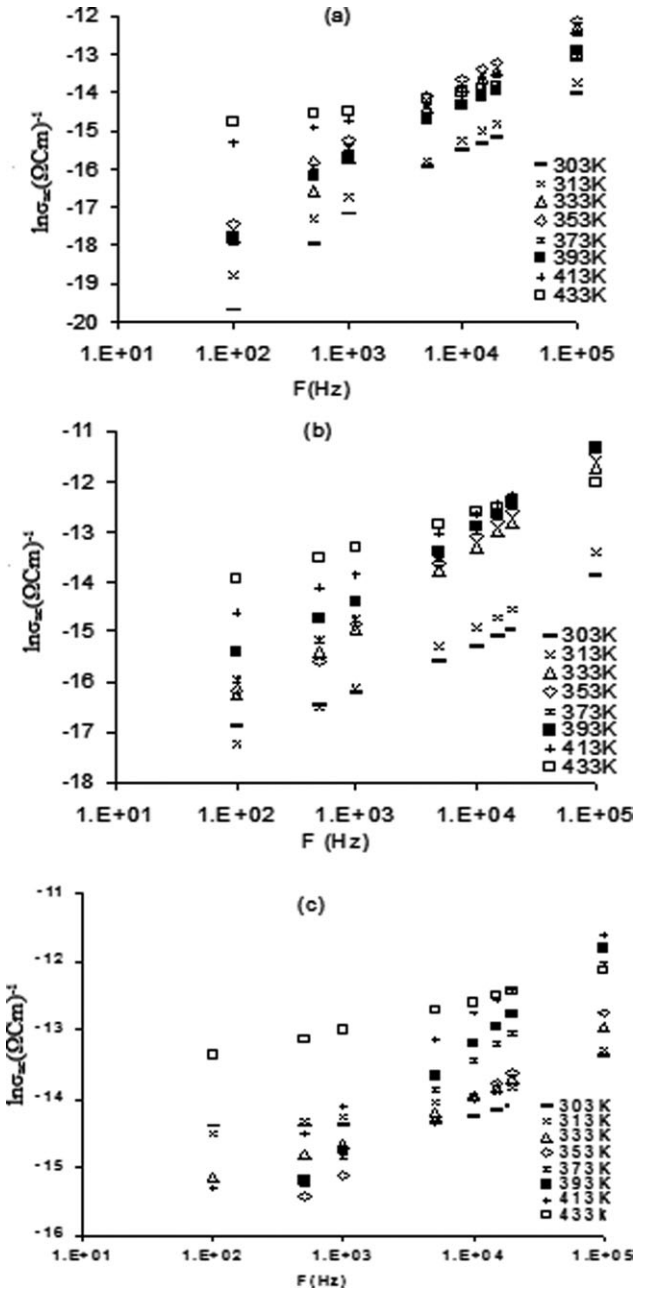

Figure 5. The frequency dependence of AC conductivity for (a) PVA/41.6wt% $CoCl_2$, (b) PVA/41.6 wt % $NiCl_2$, and (c) PVA/37.2 wt % $MnCl_2$ nanocomposites.

might be playing an important role in the conduction process. It can be noticed from these figures that more of the samples have two trend in the AC conductivity, the first one from 100 to 10 KHz is frequency independent conductivity and another from 10 to 100 KHz is frequency dependent. The first trend is contributed by free charges available in the composite system whereas the second is due to trapped charges which are only active at higher frequency region.[19] Frequency dependence of the total conductivity could be given by the following relation,[20]

$$\sigma_{tot}(\omega) = \sigma_{dc} + \sigma_{ac} = \sigma_{dc} + \mathrm{A}\omega^s \tag{6}$$

where σ_{dc} is a frequency independent term representing the DC component, A is the frequency independent factor, $\omega = 2\pi f$ is the angular frequency and the frequency exponent s ($0 < S < 1$). In most cases, the frequency dispersion of σ_{dc} has been observed to follow a universal power law of AC conductivity: $\sigma_{dc} = A\omega^s$. The determination of AC conduction mechanism implies the study of the exponent s as a function of temperature. The values of the exponent s were calculated for all investigated samples and listed in Table III. The values of s for all investigated samples lie in the range $0 < S < 1$. All samples showed the same trend at relatively low content of metal chlorides where s decreases by increasing temperature. The observed behavior of s (T) allows one to concluding that, the correlated barrier hopping (C.B.H) is the possible conduction mechanism.[21] Moreover it is observed from this table that the samples of higher concentration show the same trend where the exponent s first increases by increasing the temperature. This increase can be understood according to the quantum mechanical tunneling model (QMT).[22]

Dielectric Properties

Frequency Dependence of the Dielectric Parameters. The dependence of the dielectric permittivity ε' on frequency at various constant temperatures for PVA/metal chlorides nanocomposite samples shows a gradually decrease in ε' with increasing frequency for all prepared samples and attains a constant value at higher frequencies. This decrease of ε' with increasing frequency is the expected behavior in most dielectric materials. This behavior can be described by the Debye dispersion relation,[23]

$$\varepsilon' = \varepsilon'_{\infty} + \frac{(\varepsilon'_s - \varepsilon'_{\infty})}{1 + \omega^2\tau^2} \tag{7}$$

where ε'_s and ε'_{∞} is the static and infinite dielectric constant respectively and τ is the dielectric relaxation time. The low frequency dispersion region is attributed to the charge accumulation at the electrode–sample interface. At higher frequencies the periodic reversal of the electric field occurs so fast that there is no excess charge carriers diffusion in the direction of the field. As the frequency increases the dipoles are less able to rotate and maintain phase with the field. Thus, they reduce their contribution to the polarization field, and hence the observed reduction in the real part ε'. The variation of the dielectric loss ε'' versus frequency at various constant temperatures for PVA/metal chlorides nanocomposite samples shows that the dielectric loss ε'' decreases with increasing frequency for all samples. This behavior can be described by the Debye dispersion relation,[23]

$$\varepsilon'' = \frac{(\varepsilon'_S - \varepsilon'_{\infty})\omega\tau}{1 + \omega^2\tau^2} \tag{8}$$

where the interfacial polarization dominates[24] at relatively low frequency range which competes the normal behavior (the rise of ε'' with increasing frequency). This leads to diminish the low frequency behavior. Furthermore, as the frequency increases many types of losses get to reduce because the field frequency begins to exceed their characteristic natural frequency. This is because, for polar materials, the initial value of dielectric parameters is high, but as the frequency of the field is raised the value begins to drop which could be due to the dipoles not being able to follow the field variation at higher frequencies and also due to the polarization effects. Figure 6 shows the frequency dependence of dielectric loss tangent tan δ versus frequency at different temperatures for PVA/41.6 wt % metal chloride nanocomposites as representative diagram. From the graphs, it can be noticed that tan δ tend to decrease with increasing frequency. This attenuation of tan δ by increasing frequency can be attributed to the phonon dipole interaction which leads to a lowering of the energy transferred to the dielectric medium; this behavior characterizes amorphous polymers. Also, as the frequency increases the dipoles polarization tends to zero and tan δ depend only on electronic polarization.[25]

Table III. The Obtained Values of the Exponent (s) at Different Temperature for All PVA/Metal Chloride Nanocomposites Samples

Metal chloride content (wt %)	303 K	313 K	333 K	353 K	373 K	393 K	413 K	433 K
PVA /$CoCl_2$								
4.5	0.84	0.64	0.43	0.38	0.21	0.14	0.08	0.04
19.2	0.71	0.66	0.5	0.53	0.48	0.38	0.28	0.21
32.2	0.63	0.44	0.69	0.69	0.63	0.54	0.44	0.34
41.6	0.64	0.66	0.68	0.69	0.65	0.6	0.41	0.36
PVA /NiCl2								
4.5		0.89	0.26	0.24	0.16	0.06	0.04	0.02
19.2			0.49	0.59	0.42	0.4	0.21	0.46
32.2	0.49	0.56	0.68	0.72	0.73	0.75	0.63	0.41
41.6	0.42	0.54	0.67	0.71	0.68	0.6	0.48	0.26
PVA/$MnCl_2$								
3.8	0.78	0.55	0.48	0.39	0.26	0.18	0.15	0.08
16.5	0.81	0.63	0.59	0.56	0.47	0.37	0.3	0.24
28.3	0.39	0.44	0.25	0.35	0.49	0.52	0.37	0.34
37.2	0.12	0.16	0.31	0.48	0.58	0.64	0.55	0.18

Applied Polymer SCIENCE

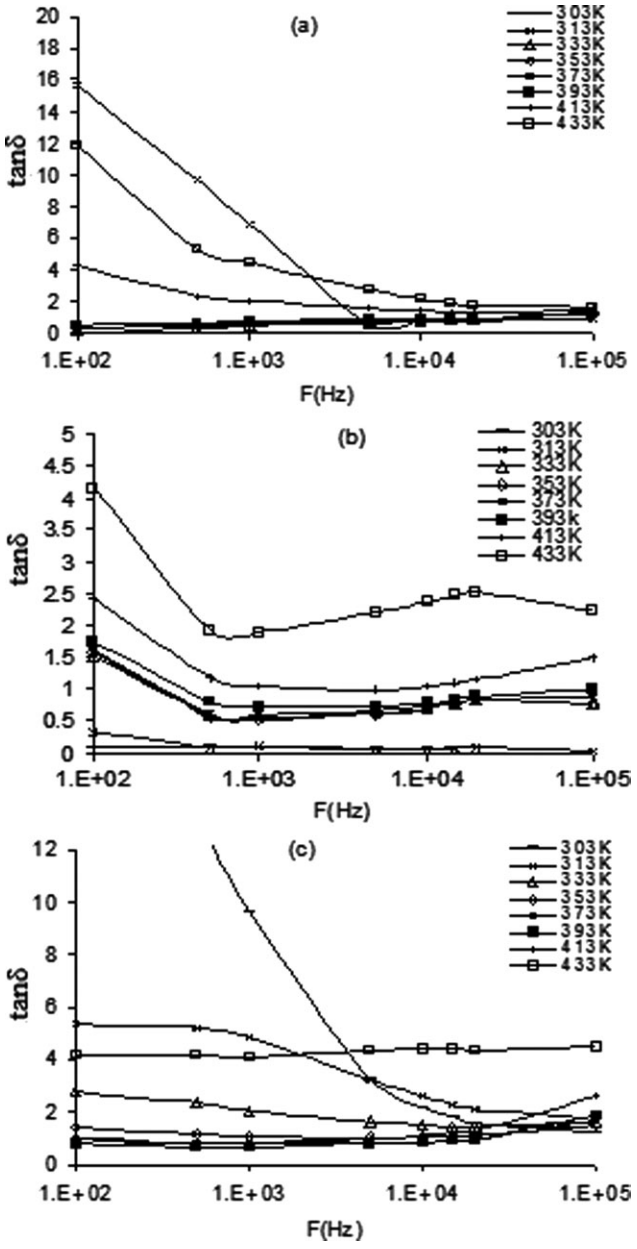

Figure 6. Dependence of loss factor on frequency at different temperature for (a) PVA/41.6 wt % $CoCl_2$, (b) PVA/41.6 wt % $NiCl_2$, and (c) PVA/37.2 wt % $MnCl_2$ nanocomposites.

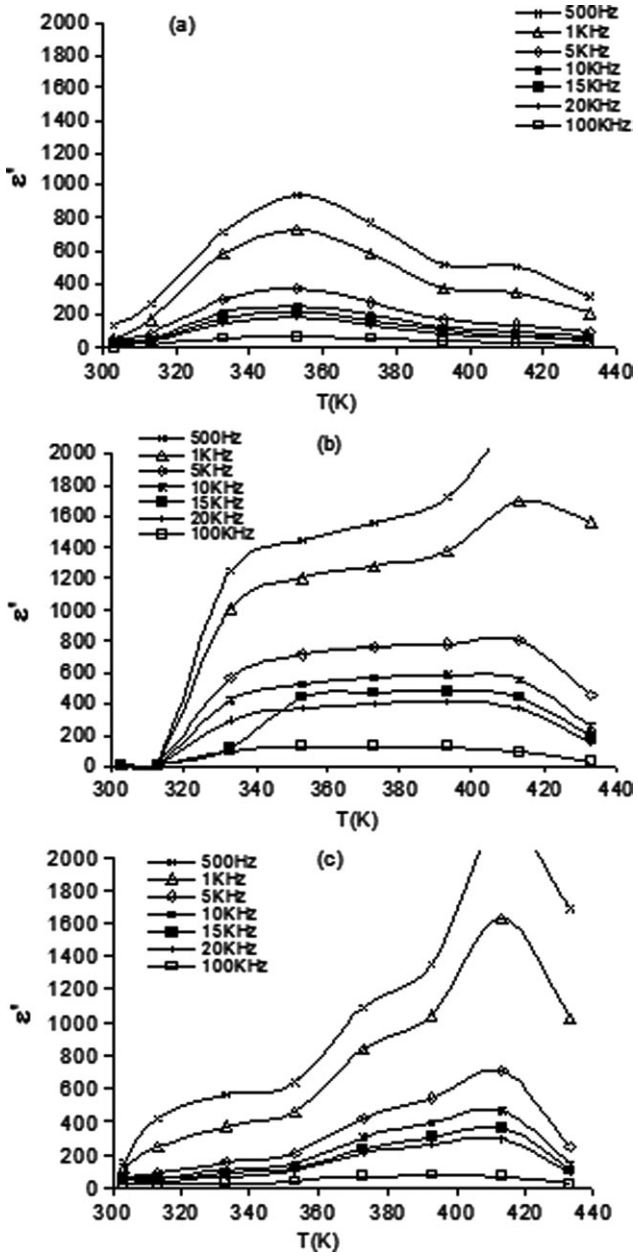

Figure 7. Dependence of dielectric constant on temperature at different frequency for (a) PVA/41.6 wt % $CoCl_2$, (b) PVA/41.6 wt % $NiCl_2$, and (c) PVA/37.2 wt %$MnCl_2$ nanocomposites.

Temperature Dependence of the Dielectric Parameters. Figure 7(a) illustrates the dependence of ε' on temperature at different constant frequencies for PVA/41.6 wt % $CoCl_2$ sample. The two peaks which observed at about 353 and 413 K are denoted as α1 and α2, respectively. The first (α1) is due to the glass transition (T_g) of the amorphous region. The second (α2) may be due to the release of the frozen dipoles and their cooperative motion with adjoining segments of the main chains, which at this temperature start to rearrange their conformations or it may be due to the decrease in the internal viscosity of the system helping the orientational polarization to occur with higher order at this high temperature. In case of PVA/41.6 wt % $NiCl_2$ sample, the peak due to the α-relaxation process associated with T_g disappear and only α2 appear around 413 K as shown in Figure 7(b). For PVA/37.2 wt % $MnCl_2$ the two relaxation peaks α1, α2 appeared at 333 and 413 K, respectively. Above (α2), the thermal energy will be sufficient to disturb the orientational dipoles and ε' is decreased.[26]

Generally, in the first temperature region, the value of ε' increases slightly up to the glass transition temperature (T_g) due to the increase in the polarization of the segmental parts of the polymer as they are oriented by the external field accompanied by the applied frequency, also around (T_g) there is polarization of polar components with the improvement of mobility polymer, which facilitates the movement of polar fillers. Accordingly,

the orientational polarization plays a significant role in the relaxation process. As, in most polymer materials, the trapped charge carriers contribute to the total polarization, the polymer system normally contains a large numbers of trapping sites, therefore one may expect a large effect of the trapped charge carrier at the lowest frequency giving large values of ε'. The creation of a carbonyl group or the high thermal energy will cause an increase in ε' with temperature. The localized dipoles involve a high degree of dipolar orientation in PVA. The molecular chains with different mobilities try to adjust and align themselves in such a way so as to add to the polarization of the system. The higher values of ε' at high temperatures are attributed to the orientational correlation of the dipoles within the chain segments. By increasing the dopant concentration, the segmental parts need less thermal energy to be polarized by the field accompanied by the applied frequency. This will cause a shift to lower (T_g) values. Maxwell–Wagner (interfacial) polarization plays a significant role because it depends on the metal ions in the polymer sample.[13]

Optical Properties

The absorption spectra for PVA/metal chloride nanocomposites samples were recorded in the wavelength range (200–900 nm). Figure 8(a) illustrates the absorption spectrum for PVA/$NiCl_2$ samples as a representative figure. The undoped PVA has an absorption peak at 280 nm, which was due to the π–π^* transition that comes from unsaturated bonds, mainly (C=O and/or C=C) in the polymer.[27] The addition of metal chlorides in PVA introduces shift this main peak for PVA polymer and additional peaks were observed due to formation of charge transfer complexes.[28] Pure PVA has an optical band gap of 3.2 eV for direct transition, 3 eV for indirect transition and 3 eV for the absorption edge.

Abdelrazek et al.[29] reported that near the fundamental band edge, both direct and indirect transitions occur and can be observed by plotting $(\alpha h\upsilon)^{1/n}$ as a function of photon energy ($h\upsilon$), where α is the absorption coefficient, υ is the frequency and h is the Planck's constant. Concerning the optical transitions resulting from photons of energy $h\upsilon > E_g$, the present optical data can be investigated according to the following relation ship for the near edge optical absorption,[30]

$$\alpha(\upsilon)h\upsilon = A(h\upsilon - E_g)^n \tag{9}$$

where A is a constant and E_g is the optical energy band gap between the valence and the conduction bands and n is the power that characterizes the transition process. The values of the absorption coefficient α can be determined as a function of frequency using the formula,[31]

$$\alpha = 2.303 \times \frac{A}{d} \tag{10}$$

where A is the absorbance and d is the thickness of the sample under investigation. The direct optical band gaps were obtained from the linear plots of $(\alpha h\upsilon)^2$ versus $h\upsilon$ for PVA/$NiCl_2$ samples as a representative figure. The extrapolations of the lines of $(\alpha h\upsilon)^2$ versus $h\upsilon$ for which $(\alpha h\upsilon)^2 = 0$, give the direct optical band gap E_{gd} and it was listed in Table IV. Also the indirect optical band gaps E_{gi} were obtained from the linear plots of $(\alpha h\upsilon)^{1/2}$ versus $h\upsilon$ as shown in Figure 8(b) for PVA/$NiCl_2$ samples as a representative figure, and the values of E_{gi} for all PVA/metal chloride prepared samples are summarized in Table IV. It is known that plots of $(\alpha h\upsilon)^{1/2}$ and $(\alpha h\upsilon)^2$ versus $h\upsilon$ give linear dependence in one region representing one optical absorption edge, while $NiCl_2$ and $CoCl_2$ doped samples give two regions representing the two optical absorption edges. These absorption edges are characterized by lower optical energy gap E_g1 and higher energy gap E_g2: Tawansi et al.,[32] reported similar results for other polymers such as PVC films doped with $NiCl_2$. From

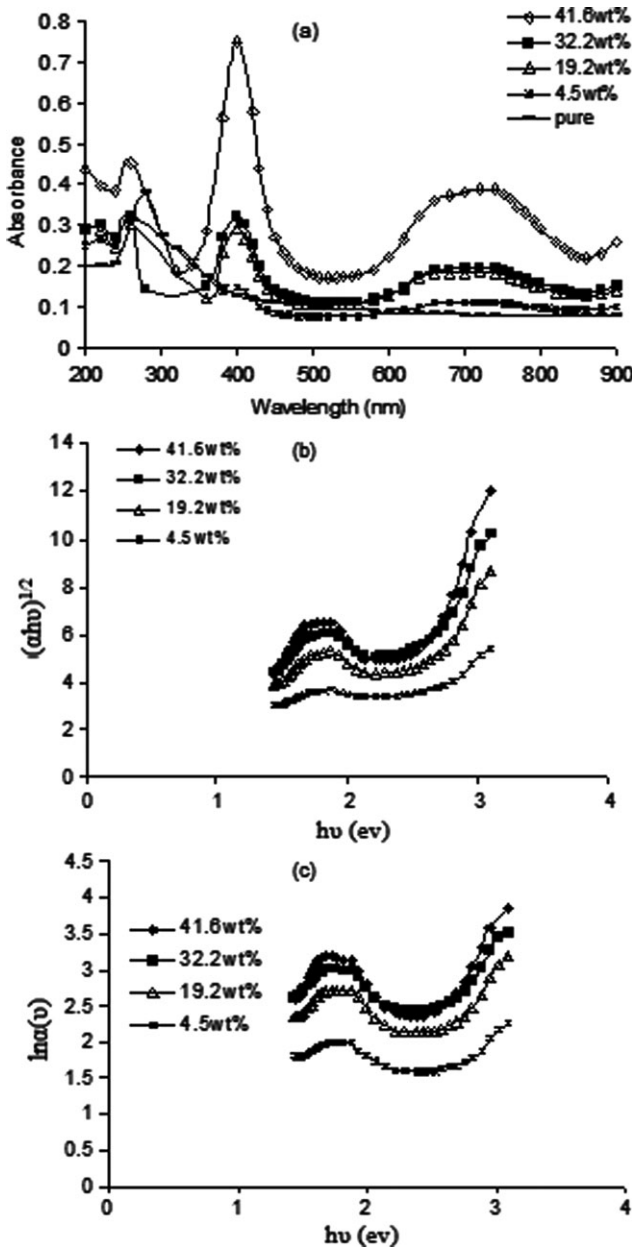

Figure 8. (a) The absorption spectra for PVA/$NiCl_2$ samples and (b and c) the dependence of $(\alpha h\upsilon)^{1/2}$ and ln (α) on the photon energy $h\upsilon$ (eV), respectively, for PVA/$NiCl_2$ samples.

Table IV. Extracted Values of the Direct E_{gd}, indirect E_{gi} Band Gap and Urbach Tail E_u for PVA/Metal Chloride Nanocomposite Samples

	Absorption edge (ev)		E_u (eV)		E_{gd} (eV; direct)		E_{gi} (ev; indirect)	
	Low energy1	High energy2	E_u1	E_u2	$E_{gd}1$	$E_{gd}2$	$E_{gi}1$	$E_{gi}2$
(a) $CoCl_2$ content (wt %)								
4.5	1.66	2.2	0.341	0.527	1.27	2.14	1.6	2.15
19.2	1.6	2.04	0.361	0.11	1.54	2.14	1.58	2.12
32.2	1.52	1.88	0.09	1.09	1.54	2.06	1.54	2.1
41.6	1.64	2.12	0.06	1.02	1.64	2.08	1.65	2
(b) $NiCl_2$ content (wt %)								
4.5	1.3	2.75	0.925	0.533	1.3	2.75	1	2.82
19.2	1.2	2.65	0.517	0.351	1.485	2.8	1.4	2.75
32.2	1.1	2.5	0.489	0.416	1.4	2.7	1.3	2.4
41.6	1.1	2.4	0.344	0.308	1.45	2.78	1.2	2.3
	Absorption edge (ev)	E_u (ev)	E_{gi} (ev)	E_{gi} (ev; indirect)				
(c) $MnCl_2$ content (wt %)								
3.8	2.95	0.268	3.6	3.25				
16.5	3.4	0.301	3.6	3.2				
28.3	2.5	0.332	3.55	3				
37.2	2.75	1.48	3.2	1.8				

this table the energy gaps for PVA contained $CoCl_2$ or $NiCl_2$ is less than that of pure PVA which is (3.2 eV) for direct transition and (3 eV) for indirect transition. The decrease in optical band gap on doping may be explained on the basis of the fact that the incorporation of amounts of dopant forms charge transfer complexes (CTCs) in the host lattice.[28] The observation of additional absorption peaks for doped films supports this view. These charge transfer complexes increase the electrical conductivity by providing additional charges in the lattice. This results in a decrease of optical band gap.[28] For $MnCl_2$ contained samples, the increase of metal chloride content have small significant changes on the optical gap width which mainly depend on the metal chloride particle size in the polymer matrix. As the size of semiconductor particles decreases to the nanoscale, the band gap of the semiconductor increases, causing a blue shift in the UV–vis absorption spectra due to quantum confinement.[33] Conversely, for optical transitions caused by photons of energy $h\upsilon < E_g$, the absorption of photons is related to the presence of localized tail states in the forbidden gap. The width of this tail, called the Urbach tail, is an indicator of the defect levels in the forbidden band gap. Urbach assumed that the absorption coefficient near the band edge shows exponential dependence on photon energy according to the following relation,[34]

$$\alpha = \alpha_o \exp\left(\frac{h\upsilon}{E_u}\right) \tag{11}$$

where α_o is constant, E_u is the Urbach's energy corresponding to the width of the band tails of the localized states in the band gap. These are formed as a result of extrinsic origins arising from defects or impurities, to extended states in the conduction bands. The values of E_u were estimated using the least square fitting of eq. (11). Figure 8(c) shows the relation between $Ln(\alpha)$ versus photon energy $h\upsilon$ for PVA/$NiCl_2$ samples. The position of the absorption edge was determined by extrapolating the linear portions of the $Ln(\alpha)$ versus photon energy $h\upsilon$ curves and listed in Table IV. The extracted values of E_u are listed in Table IV. The variation of the magnitude of E_u of polymer composites can be understood by considering the mobility concept that filling significantly affects the Urbach energy E_u as proposed by Davis and Mott.[35] The process of filling introduces additional defect states in the polymeric matrix. The density of localized states was found to be proportional to the concentration of these defects and consequently to metal chlorides and free ions contents.[34] The increase of salt ratio content may cause the localized states of different color centers to overlap and extend in the mobility gap.[36] This overlap may provide evidence of the considerable change in E_u when salt ratio is increased in the polymeric matrix. From Table IV one can noticed that the magnitudes of E_a which obtained from DC conductivity data are small in comparison with optical band gap energies E_{gi} or E_{gd}. This is due to the fact that their nature is different. Although the activation energy corresponds to the energy required for conduction from one site to another, the optical band gap corresponds to interband transition.

CONCLUSION

PVA/metal chloride nanocomposites were prepared. XRD, DSC, and SEM confirmed the change in the PVA structure with the addition of metal chlorides. Activation energy values obtained from the DC conductivity measurements were found in the range from 0.64 to 0.26 eV for all investigated samples. This type of composites could thus be a suitable candidate for electronic application, although a further enhancement in conductivity, especially at the lowest temperature, is desired. The AC conductivity obeyed the ω^s power law. The behavior of s with

temperature interpreted on the basis of correlated barrier hopping and quantum mechanical tunneling models. The dielectric parameters were found to decreases with increasing frequency. The study of dielectric relaxation as a function of temperature at constant frequency shows two types of relaxation processes. The optical absorption measurements indicate that the absorption mechanism is due to allowed direct and indirect transitions for the composites. It is evaluated that the optical band gap and Urbach energy values changes with the change in both particle size of metal chlorides and its concentration inside the polymer matrices which due to quantum confinement.

REFERENCES

1. Liwei, Z. M.Sc. Thesis, Duke University, **2010**.
2. Tawansi, A.; Zidan, H. M.; Oraby, A. H.; Dorgham, M. E. *J. Phys. D: Appl. Phys.* **1998**, *31*, 3428.
3. Mbhele, Z. H.; Salemane, M. G.; van Sittert, C. G. C. E.; van Sittert, J. M. W.; Djoković, V. *Chem. Mater.* **2003**, 15, 5019.
4. Qian, X. F.; Yin, J.; Guo, X. X.; Yang, Y. F.; Zhu, Z. K.; Lu, J. *J. Mater. Sci. Lett.* **2000**, *19*, 2235.
5. Radheshkumar, C.; Münstedt, H. *Mater. Lett.* **2005**, *59*, 1949.
6. Espuche, E.; David, L.; Rochas, C.; Afeld, J. L.; Compton, J. M.; Thompson, D. W.; Kranbuehl, D. E. *Polymer* **2005**, *46*, 6657.
7. Zidan, H. M. *Polym. Test.* **1999**, *18*, 449.
8. El-Khodary, A.; Oraby, H. A.; Abdelnaby, M. M. *J. Magn. Magn. Mater.* **2008**, *320*, 1739.
9. Hodge, R. M.; Edward, G. H.; Simon, G. P. *Polymer* **1996**, *37*, 1371.
10. Kitazawa, S.; Choi, Y.; Yamamoto, S.; Yamaki, T. **2006**, *515*, 1901.
11. Abdelrazek, E. M.; Elashmawi, I. S.; El-khodary, A.; Yassin, A. *Curr. Appl. Phys.* **2010**, *10*, 607.
12. Bhajantri, R. F.; Ravindrachary, V.; Harisha, A.; Crasta, V.; Nayak, P. S. Poojary, B. *Polymer* **2006**, *47*, 3591.
13. Seanor, D. A. Electerical Properties of Polymers; Academic press: New York, **1982**.
14. El-Tantawy, F.; Abdel-Kader, K. M.; Kaneko, F.; Sung, Y. K. *Eur. Polym. J.* **2004**, *40*, 415.
15. El-Tantawy, F.; Kamada, K.; Ohnabe, H. *Polym. Int.* **2002**, *51*, 635.
16. Psarras, G. C. *Compos. Part A* **2006**, *37*, 1545.
17. Li Shao, H.; Okui, N. *Polym. J.* **1999**, *31*, 1083.
18. El-Tantawy, F. *Eur. Polym. J.* **2001**, *37*, 565.
19. Harun, M. H.; Saion, E.; Kassim, A.; Hussain, M. Y.; Mustafa, I. S.; Omer, M. A. A. *Malaysian Polym. J.* **2008**, *3*, 27.
20. El Mansy, M. K. *Mater. Chem. Phys.* **1998**, *56*, 238.
21. Elliott, S. R. *Philos. Mag.* **1977**, *36*, 1291.
22. Elliot, S. R. *Adv. Phys.* **1987**, *36*, 135.
23. Debye, P. Polar Molecules; Dover: NewYork, **1945**.
24. Jonscher, A. K. *Nature* **1977**, *267*, 673.
25. Shash, N. M. *J. Appl. Polym. Sci.*, to appear.
26. Ahmed, M. A.; Abo-Ellil, M. S. *Mater. Electron.* **1998**, *9*, 391.
27. Abdelrazek, E. M. *Phys. B* **2008**, *403*, 2137.
28. Uma Devi, C.; Sharma, A. K.; Rao, V. V. R. N. *Mater. Lett.* **2002**, *56*, 167.
29. Abdelrazek, E. M.; Elashmawi, I. S.; El-khodary, A.; Yassin, A. *Curr. Appl. Phys.* **2010**, *10*, 607.
30. Aydogdu, Y.; Yakuphanoglu, F.; Aydogdu, A.; Tas, E.; Cukuraval, A. *Solid State Sci.* **2002**, *4*, 879.
31. Elashmawi, I. S.; Hakeem, N. A. *Polym. Eng. Sci.* **2008**, *895*, 48.
32. Tawansi, A.; Zidan, H. M.; Mostafa, Y. M.; Eldumiatty, A. H. *Phys. Script.* **1997**, *55*, 243.
33. Wang, H.; Fang, P.; Chen, Z.; Wang, S. *Appl. Surf. Sci.* **2007**, *253*, 8495.
34. Urbach, F. *Phys. Rev.* **1953**, *92*, 1324.
35. Davis, E. A.; Mott, N. F. *Philos. Mag.* **1970**, *22*, 903.
36. Dow, J. D.; Redfield, D. *Phys. Rev. B.* **1972**, *5*, 594.